Comparisons of wild-type and mutant flavodoxins from Anacystis nidulans. Structural determinants of the redox potentials

ARTICLE *in* JOURNAL OF MOLECULAR BIOLOGY · DECEMBER 1999

Impact Factor: 4.33 · DOI: 10.1006/jmbi.1999.3152 · Source: PubMed

7 AUTHORS, INCLUDING:

David Hoover
National Institutes of Health
31 PUBLICATIONS **2,763** CITATIONS
SEE PROFILE

Anita L Metzger
University of Michigan
8 PUBLICATIONS **583** CITATIONS
SEE PROFILE

Chris Weber
University of Michigan
14 PUBLICATIONS **716** CITATIONS
SEE PROFILE

Katherine A Pattridge
University of Michigan
20 PUBLICATIONS **1,338** CITATIONS
SEE PROFILE

Article No. jmbi.1999.3152 available online at http://www.idealibrary.com on IDEAL® J. Mol. Biol. (1999) 294, 725–743

JMB

Comparisons of Wild-type and Mutant Flavodoxins from *Anacystis nidulans*. Structural Determinants of the Redox Potentials

David M. Hoover, Catherine L. Drennan, Anita L. Metzger, Charles Osborne, Christian H. Weber, Katherine A. Pattridge and Martha L. Ludwig*

Biophysics Research Division and Department of Biological Chemistry, University of Michigan, 930 N. Univeristy Ave., Ann Arbor, MI 48109, USA

The long-chain flavodoxins, with 169-176 residues, display oxidation-reduction potentials at pH 7 that vary from −50 to −260 mV for the oxidized/semiquinone (ox/sq) equilibrium and are −400 mV or lower for the semiquinone/hydroquinone (sq/hq) equilibrium. To examine the effects of protein interactions and conformation changes on FMN potentials in the long-chain flavodoxin from *Anacystis nidulans* (*Synechococcus* PCC 7942), we have determined crystal structures for the semiquinone and hydroquinone forms of the wild-type protein and for the mutant Asn58Gly, and have measured redox potentials and FMN association constants. A peptide near the flavin ring, Asn58-Val59, reorients when the FMN is reduced to the semiquinone form and adopts a conformation (''O-up'') in which O 58 hydrogen bonds to the flavin N(5)H; this rearrangement is analogous to changes observed in the flavodoxins from *Clostridium beijerinckii* and *Desulfovibrio vulgaris*. On further reduction to the hydroquinone state, the Asn58-Val59 peptide in crystalline wild-type *A. nidulans* flavodoxin rotates away from the flavin to the ''O-down'' position characteristic of the oxidized structure. This reversion to the conformation found in the oxidized state is unusual and has not been observed in other flavodoxins. The Asn58Gly mutation, at the site which undergoes conformation changes when FMN is reduced, was expected to stabilize the O-up conformation found in the semiquinone oxidation state. This mutation raises the ox/sq potential by 46 mV to −175 mV and lowers the sq/hq potential by 26 mV to −468 mV. In the hydroquinone form of the Asn58Gly mutant the C-O 58 remains up and hydrogen bonded to N(5)H, as in the fully reduced flavodoxins from *C. beijerinckii* and *D. vulgaris*. The redox and structural properties of *A. nidulans* flavodoxin and the Asn58Gly mutant confirm the importance of interactions made by N(5) or N(5)H in determining potentials, and are consistent with earlier conclusions that conformational energies contribute to the observed potentials.

The mutations Asp90Asn and Asp100Asn were designed to probe the effects of electrostatic interactions on the potentials of protein-bound flavin. Replacement of acidic by neutral residues at positions 90 and 100 does not perturb the structure, but has a substantial effect on the sq/hq equilibrium. This potential is increased by 25-41 mV, showing that electrostatic interaction between acidic residues and the flavin decreases the potential for conversion of the neutral semiquinone to the anionic hydroquinone. The potentials and the effects of mutations in *A. nidulans* flavodoxin are rationalized using a thermodynamic scheme developed for *C. beijerinckii* flavodoxin.

D. M. Hoover and C. L. Drennan contributed equally to this work.

Present addresses: C. L. Drennan, Dept. Chemistry, Massachusetts Institute of Technology, Cambridge, MA 02139 USA; D. M. Hoover, Protein Structure Section, National Cancer Institute, Frederick, MD 21702, USA.

Abbreviations used: ox/sq, oxidized/semiquinone; sq/hq, semiquinone/hydroquinone.

E-mail address of the corresponding author: ludwig@biop.umich.edu

0022-2836/99/480725–19 $30.00/0

Keywords: flavodoxin; redox potentials; FMN binding; flavin semiquinone; flavin hydroquinone

*Corresponding author

Introduction

Flavodoxins act as one-electron carriers in a variety of reactions (Mayhew & Tollin, 1992). To facilitate these reactions, the reduction potentials of FMN bound to flavodoxin are perturbed, relative to those of free FMN, so that flavodoxin can be reduced in two discrete one-electron steps†. The effects of protein interactions on the potentials for the oxidized/semiquinone (ox/sq) equilibrium, $E_{ox/sq}$, vary somewhat with the species of flavodoxin, but the potentials for addition of the second electron, $E_{sq/hq}$, are all much below the values for free FMN and are typically −400 mV or lower at pH 7.0 (Table 1). Thus a key property of these proteins, which display the lowest potentials known for protein-bound FMN or FAD, is destabilization of the fully reduced form of the flavin cofactor. In the flavodoxin from *Anacystis nidulans*, the sq/hq potential is approximately −445 mV, and the ox/sq potential is close to the value for free FMN (Figure 1). As is evident from the thermodynamic cycles shown in Figure 1, the effects of the protein on redox potentials, which correspond to free energy changes as large as 6 kcal/mol, are linked to changes in association constants. Thus the control of potentials may be understood in terms of the free energies for FMN binding and the interactions that contribute to those energies.

The ways in which flavodoxin apoproteins influence the free energies of FMN reduction have been extensively studied in the short-chain flavodoxins from *Clostridium beijerinckii* (Ludwig & Luschinsky, 1992; Ludwig *et al*., 1990, 1997) and *Desulfovibrio vulgaris* (Mayhew *et al*., 1996; Swenson & Krey, 1994; Watt *et al*., 1991; Zhou & Swenson, 1995, 1996a). Comparisons of the structures of oxidized and semiquinone forms of *C. beijerinckii* flavodoxin have revealed a conformation change that accompanies introduction of the first electron (Smith *et al*., 1977). A peptide in the ''50's loop'', a turn that adjoins the flavin ring, rearranges to what we call the O-up conformation, in which the backbone oxygen atom is hydrogen bonded to the N(5)H of the neutral FMN semiquinone. This new interaction between the protein and the prosthetic group is an important feature that favors formation of the semiquinone and increases the ox/sq redox potential (Ludwig *et al*., 1997). As revealed by the structures we now describe, related conformation changes occur in *A. nidulans* flavodoxin. A peptide flip and hydrogen bonding rearrangement also accompany reduction of oxidized *D. vulgaris* flavodoxin (Watenpaugh *et al*., 1973; Watt *et al*., 1991). In both *C. beijerinckii* and *D. vulgaris* flavodoxins site mutations have been targeted to the 50's loops to study the connection between loop conformation and the energetics of reduction (Ludwig *et al*., 1997; Mayhew *et al*., 1996; O'Farrell *et al*., 1998).

In flavodoxins from *C. beijerinckii* or *D. vulgaris*, further reduction to the hydroquinone does not change the 50's loop; the hydrogen bond at N(5)H remains intact and no conformation changes occur on addition of the second electron. Thus protein rearrangements are not a primary determinant of the sq/hq potential. For a time it was presumed that the protein held the reduced isoalloxazine ring in an unfavorable planar conformation, and that the resulting strain accounted for the low redox potential (Ludwig *et al*., 1976). However, NMR measurements (Moonen *et al*., 1984) subsequently indicated that unsubstituted free reduced flavins are essentially planar and the ring-strain rationale for the low sq/red potential was abandoned‡. Recent studies of wild-type and mutant flavodoxins from *D. vulgaris* (Zhou & Swenson, 1995), *C. beijerinckii* (Ludwig *et al*., 1990) and *Anabaena* (Lostao *et al*., 1997) have focused on electrostatic effects that influence the sq/hq potentials. The ^{15}N chemical shifts of the flavin N(1) in these flavodoxins indicate that the protein-bound reduced flavin is anionic§, and not protonated at N(1) (Franken *et al*., 1984; Stockman *et al*., 1988; Vervoort *et al*., 1986). In flavodoxins for which structures are known, the negative charge distributed on the reduced isoalloxazine ring (Hall *et al*., 1987c; Zheng & Ornstein, 1996) is surrounded by a partly hydrophobic environment including a number of Asp and Glu residues but lacking compensating countercharges. The contribution of electrostatic repulsion to the sq/hq potential of *D. vulgaris* flavodoxin has been estimated from a series of individual and multiple mutations

† An interesting exception to this rule is the behavior of the flavodoxin-like domain of P450BM-3 (Sevrioukova *et al*., 1996).

‡ Molecular orbital calculations have found modest potential energy barriers to ring flattening in neutral reduced flavins (Dixon & Lipscomb, 1979; Hall *et al*., 1987ab; Zheng & Ornstein, 1996). Recent calculations find the anionic reduced flavin to be essentially planar (Zheng & Ornstein, 1996).

§ Yalloway *et al*. (1999) have re-examined the ionization of reduced FMN in *Megasphaera elsdenii* and *D. vulgaris* flavodoxins and concluded that the anionic isoalloxazine is converted to a neutral (uncharged) species with pK_a values of 5.8 and 6.5. It is not clear how to reconcile these observations with the NMR measurements, which indicate that N(1) remains unprotonated at lower pH values.

Table 1. Redox potentials of flavodoxins at pH 7.0 in mV

Source[a]	E_2(ox/sq)	E_1(sq/hq)	E_m^b(ox/hq)	Reference
A. Long-chain flavodoxins				
Anabaena 7120*	−196	−425	−310	Paulsen *et al.* (1990)
*Anacystis nidulans**	−221	−447	−334	Entsch & Smillie (1972)
	−215	−414	−315	Sykes & Rogers (1984)
	−221	−442	−330	This work
Azotobacter chroococcum	−103	−522	−312	Deistung & Thorneley (1986)
Azotobacter vinelandii[c]	−228	−464	−346	Yoch (1972)
	−165	−458	−311	Taylor *et al.* (1990)
*Chondrus crispus**	−222	−370	−296	Sykes & Rogers (1984)
*Escherichia coli**	−244	−455	−349	Vetter & Knappe (1971)
	−260	−452	−356	Hoover & Ludwig (1997)
Klebsiella pneumoniae	−170	−422	−296	Deistung & Thorneley (1986)
Synechococcus lividus	−50	−450	−250	Crespi *et al.* (1972)
B. Short chain flavodoxins				
*Clostridium beijerinckii**	−92	−399	−245	Mayhew (1971)
Clostridium pasteurianum	−132	−419	−275	Mayhew (1971)
*Desulfovibrio vulgaris**	−143	−440	−291	Curley *et al.* (1991)
*Desulfovibrio desulfuricans**	−58	−387	−222	Caldeira *et al.* (1994)
*Megasphaera elsdenii**	−115	−372	−243	Mayhew *et al.* (1969)
FMN	−238	−172	−205	Draper & Ingraham (1968)
	−314	−124	−219	Anderson (1983)

Some potentials were not measured at pH 7.0. For these, a −59 mV change per pH unit was used to estimate E_2 at pH 7.0. It was assumed that E_1 values did not change at pH values above 7.0.

[a] An asterisk (*) indicates that the three-dimensional structure has been determined.

[b] E_m is the overall midpoint potential calculated by averaging E_1 and E_2.

[c] Additional values have been reported for the potential of *A. vinelandii* flavodoxin by Barman & Tollin (1972), and Klugkist *et al.* (1986). Several flavodoxins with differing potentials have been isolated from strains ATCC 478 and OP (Mayhew & Tollin, 1992; Steensma *et al.*, 1996). Values from Taylor *et al.* (1990) are for the recombinant, dephospho enzyme.

(Swenson & Krey, 1994; Zhou & Swenson, 1995, 1996a).

The long-chain flavodoxins are distinguished from the short-chain *C. beijerinckii* flavodoxin by the insertion of approximately 20 residues in the fifth strand of the central parallel sheet, and by differences in the 50's and 90's loops that contact the FMN (Drennan *et al.*, 1999). These larger flavodoxins typically display ox/sq and sq/hq potentials that are lower than those of *C. beijerinckii* flavodoxin (see Table 1). *A. nidulans* flavodoxin has an ox/sq potential of −221 mV, a value not very different from that for free FMN, and 130 mV (+3.0 kcal/mol) below the ox/sq potential of *C. beijerinckii* flavodoxin. The potential for the sq/hq equilibrium is −442 to −447 mV (Entsch & Smillie, 1972; this work), about 50 mV below the potential for *C. beijerinckii* flavodoxin. As described here, structures of the semiquinone and hydroquinone forms of *A. nidulans* flavodoxin have been determined to ascertain how the conformations of the FMN binding site and 50's loop change with oxidation state in this long-chain flavodoxin. The mutant Asn58Gly was constructed to assess the effects of the Asn side-chain on redox potentials and on the peptide conformation at 58-59. Substitutions of Asp90 and Asp100 by Asn were designed to estimate the magnitudes of electrostatic interactions in reduced *A. nidulans* flavodoxin. The structural and functional data from wild-type and mutant *A. nidulans* flavodoxins explore the mechanisms that control potentials in this flavodoxin and in the closely related long-chain flavodoxins from *Escherichia coli* and *Anabaena*.

Results

Structures of the semiquinone and hydroquinone oxidation states of wild-type *A. nidulans* flavodoxin and of the Asn58Gly mutant were determined by alternating refinement in X-PLOR (Brünger, 1992) with model building, starting from models for the corresponding oxidized forms (Drennan *et al.*, 1999). Crystallographic data are summarized in Table 2 and refinement statistics are shown in Table 3. Structures of the oxidized forms of the Asp90Asn and Asp100Asn mutants were similarly determined to ensure that these residue substitutions removed a formal negative charge without perturbing the three-dimensional geometry of the FMN binding site. Final R values ranged from 0.157 to 0.167 for data extending to an outer resolution of 1.90 to 1.80 Å. Oxidation-reduction potentials of the mutants were measured to correlate potential shifts with the observed structures.

The structure of the semiquinone form of *A. nidulans* flavodoxin

For analysis of the semiquinone form at 1.8 Å resolution, intensities were measured from form II

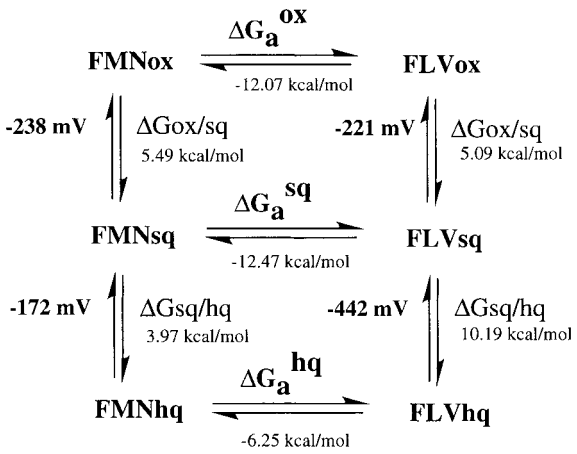

Figure 1. Thermodyamic cycles connecting oxidation-reduction potentials and association constants for flavodoxin from *A. nidulans* at pH 7.0. Free energies are for association and reduction respectively. The perturbation of the potentials by the protein and the changes in association constant with redox state are equivalent measures of the flavin:protein interactions. Association constants for the semiquinone and hydroquinone states have been calculated from the measured potentials and the experimental value of K_a for oxidized flavodoxin. In similar measurements on *Anabaena* flavodoxin, Lostao *et al.* (1997) determined a ΔG of -14.2 kcal/mol for binding of oxidized FMN and calculated from the measured ox/hq potential of -324 mV a ΔG of -8.7 kcal/mol for binding of the hydroquinone form.

crystals because their chunkier habit provided a larger X-ray scattering volume (Table 2; Drennan *et al.*, 1999). In maps calculated with the higher resolution data we expected to find features demonstrating a change in conformation at the Asn58-Val59 peptide. At first sight the difference maps, computed with coefficients $(|F_{sq}| - |F_{ox}|)\exp i\alpha_{ox}$, were puzzling. Strong difference densities indicated significant displacements at Val59, but features at the atoms of the Asn58-Val59 peptide were much weaker (Figure 2).

Refinement of the structure of the semiquinone form verified that peptide rotation had indeed occurred. Positional refinement was carried out in X-PLOR (Brünger, 1992) with residues 57-60 omitted from the model, and models of the O-up and O-down conformations (Figure 2) were fit to omit map density using TOM (Cambillau & Horjales, 1987; Jones & Thirup, 1986). The two models were subjected to further rounds of refinement, including simulated annealing and refinement of individual atom *B*-factors (Drennan *et al.*, 1999). After refinement of the model with O 58-up, there was no significant $(|F_o| - |F_c|)$ difference density to suggest that the peptide was incorrectly oriented. However, after refinement with O 58-down, negative difference density appeared at the carbonyl oxygen atom of Asn58, and positive difference density was observed at the O-up location. Difference maps calculated after a full round of omit refinement (Drennan *et al.*, 1999) that started with the final parameters (Table 3, $R = 0.165$) confirmed the assignment of the O 58-up conformation.

When the refined semiquinone and oxidized conformations are superimposed, the original difference map, with coefficients $(|F_{sq}| - |F_{ox}|)\exp i\alpha_{ox}$, can easily be understood. Figure 2 shows that the 57-60 loop adjusts when the peptide flips so the largest differences in atom positions occur at Val59. The distance between the C^β atom of Val59 in the oxidized structure and the C^β atom of Val59 in the semiquinone structure is 1.9 Å. The carbonyl oxygen atom of Asn58, on the other hand, moves into a location that had been partially occupied by N 59, and the nitrogen atom of 59 moves close to the position occupied by O 58 in the oxidized structure. Because the net change of atomic positions in the peptide is small, difference densities at the 58-59 peptide are weak and shifts of the Val59 atoms dominate the map (Figure 2).

The movement of Val59 is associated with the peptide flip in an intriguing way. If the Asn58-Val59 peptide turned over without an adjustment of Val59, the carbonyl oxygen atom of Asn58 would not be positioned to form a hydrogen bond

Table 2. Cell dimensions and data collection statistics

Parameter/Crystal	WT sq (form II)	WT hq (form I)	N58G sq (form III[a])	N58G hq (form III[a])	D90N ox (form II)	D100N ox (form II)
Cell *a* (Å)	59.79	57.18	50.59	50.78	60.03	60.17
Cell *b* (Å)	65.43	69.40	57.91	58.34	65.77	66.17
Cell *c* (Å)	51.51	46.04	93.39	93.50	51.43	51.41
Resolution (Å)	1.80	1.85	1.86	1.85	1.90	1.90
Unique reflections	18019	15263	22795	22650	15656	16059
% Completeness[b]	94(85)	95(88)	97(98)	94(92)	95(90)	97(90)
Redundancy	3.0	5.0	4.7	4.4	3.3	3.2
$I/\sigma(I)$ at d_{min}	2.4	3.6	2.9	2.1	3.2	2.1
R_{sym}[c]	0.054	0.048	0.059	0.067	0.044	0.064

All forms belong to space group $P2_12_12_1$.
[a] Data collected at 140 K; other data sets were collected at 4 °C.
[b] Numbers in parentheses represent values for the outermost shell of data.
[c] $R_{sym} = \Sigma_h \Sigma_i |I_i - \langle I \rangle| / \Sigma_h \Sigma_i \langle I \rangle$.

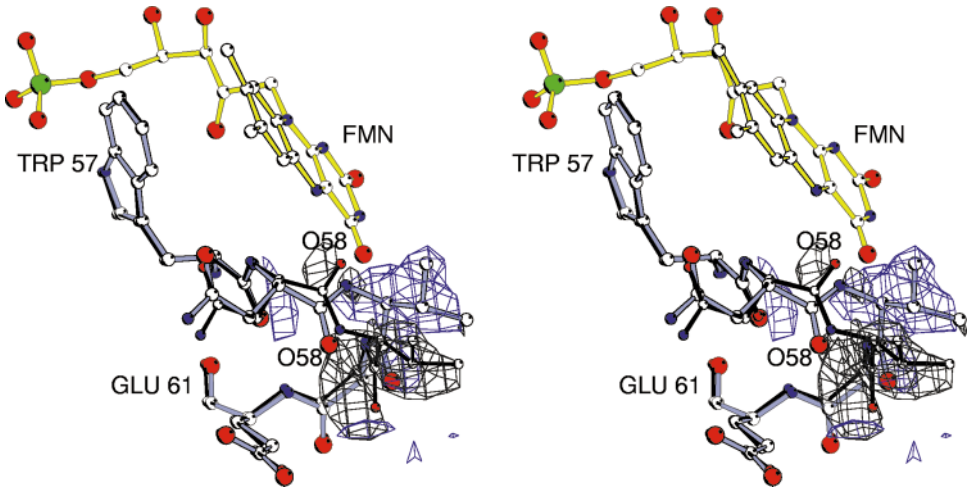

Figure 2. A stereoview of the difference map computed with coefficients $(|F_{sq}| - |F_{ox}|)$ exp $i\alpha_{ox}$. Refined models of the structures of the oxidized (O-down) and semiquinone (O-up) forms are superimposed on the difference density; the model of the oxidized form is drawn with thick blue bonds and the semiquinone model with thinner black bonds. Positive contours (3σ) are black and negative contours (−3σ) are blue. Positions of O 58-up and N 59-down almost correspond, as do positions of O 58-down and N 59-up, explaining the small difference densities at the atoms of the 57-58 peptide.

to the N(5)H of the flavin, and would be uncomfortably close to the flavin ring. As shown in Figure 2, the displacement of Val59 accommodates hydrogen bonding between the carbonyl group and the N(5)H of the FMN with an O–N distance of 2.93 Å and an O–H–N angle of 138°. The displacement also allows a switch between the N(5)–HN 59 interaction in the oxidized form and the N(5)H–O 59 hydrogen bond in the semiquinone form. The movement of the C^{α} atom of Val59 forces adjustments of the Val59 side-chain and the Val59 carbonyl group, but does not affect dramatically the position of the nitrogen atom of Gly60, which is a hydrogen bond donor to the O(4) of the FMN (Table 4). Likewise, the residues upstream of the Asn58-Val59 peptide are not much affected by the peptide inversion. The position of Trp57 is virtually unchanged, and although the C^{α} atom of Asn58 must adjust to maintain proper geometry when the peptide rotates, the movement is much less than that of Val59. Despite the several large displacements of atoms, residues 58-60 still form a three residue turn in the semiquinone structure, and the hydrogen-bonded bridge between Trp57 and Glu61 is preserved. Conformational energies associated with the observed structural rearrangements are considered in the Discussion.

The structure of the hydroquinone form of *A. nidulans* flavodoxin

Data were collected from a form I crystal that had been reduced with excess dithionite at pH 8.5 under anaerobic conditions (see Materials and Methods); the starting model was the refined structure of oxidized form I flavodoxin. By analogy

Table 3. Statistics for refined models

Parameter	WT sq (form II)	WT hq (form I)	N58G sq (form III[a])	N58G hq (form III[a])	D90N ox (form II)	D100N ox (form II)
Resolution range (Å)	10.0-1.80	10.0-1.85	10.0-1.85	10.0-1.85	10.0-1.90	10.0-1.90
R[b]	0.165	0.168	0.168	0.166	0.154	0.157
R_{free}	0.218	0.207	0.209	0.202	0.193	0.200
No. of non-H atoms						
Protein	1318	1318	1314	1314	1318	1318
Heteroatoms	31	31	48	36	31	31
Solvents	131	124	238	251	95	108
Alternate side-chains	6			9		
Average B[c] (Å^2)	19.97	17.05	13.18	12.74	14.06	12.05
RMS deviation from ideal						
Bond lengths (Å)	0.008	0.008	0.008	0.009	0.007	0.008
Bond angles (deg.)	1.374	1.310	1.329	1.364	1.281	1.381
Improper angles (deg.)	1.156	1.127	1.311	1.396	1.085	1.224

[a] Data collected at 140 K; other data sets were collected at 4 °C.
[b] No σ cutoff.
[c] Protein atoms.

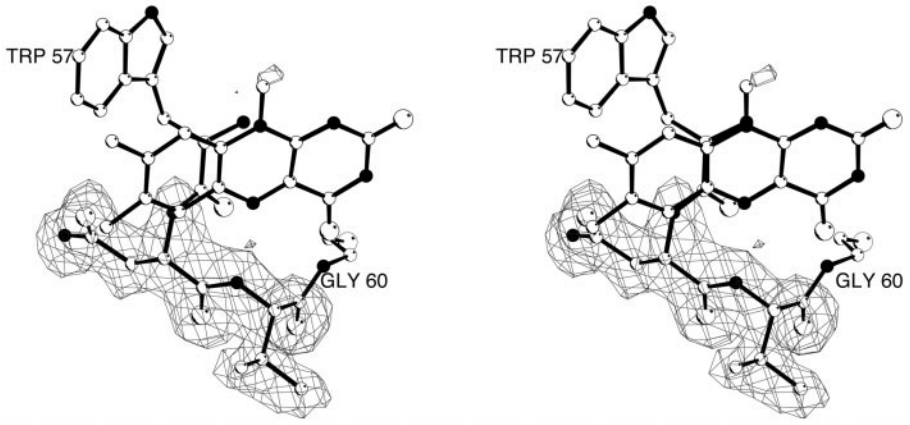

Figure 3. The hydroquinone form of wild-type *A. nidulans* flavodoxin. Contours at 3σ are from a difference Fourier map calculated with amplitudes ($|F_o| - |F_c|$) after a final simulated annealing refinement that omitted residues 58-59. The Φ,Ψ angles at Asn58 and Val59 are (42, 48°) and (66, 77°). (see Table 6). As in all the other black-and-white illustrations, nitrogen atoms are filled and carbon atoms are open; oxygen atoms are drawn with larger radii.

with flavodoxin from *C. beijerinckii*, we expected to find the peptide connecting Asn58 and Val59 in the O-up conformation, oriented to form a hydrogen bond to the N(5)H of FMN. However the initial difference maps, computed with coefficients $(|F_{hq}| - |F_{ox}|)\exp i\alpha_{ox}$, displayed no strong features in the vicinity of Asn58-Val59, suggesting that these residues adopted similar conformations in the oxidized and hydroquinone forms, with O 58-down in the hydroquinone state. Density shapes in maps where residues 57-60 were omitted from the phasing also corresponded closely to the O-down conformation for O 58. These results were not attributable to reoxidation of the crystal: visual inspection showed that it remained almost colorless throughout data collection, and epr measurements after data collection verified that reoxidation had been minimal (Luschinsky *et al.*, 1991).

Further rounds of refinement of the atomic model *versus* the data from the reduced crystal, using simulated annealing in X-PLOR (Brünger *et al.*, 1990), were carried out to examine the conformation of residues 58-59. When the model was refined with the 58-59 peptide in the O-down conformation, no difference density peaks were associated with the 58-59 peptide. On the other hand, when the peptide was modeled in the O-up position, there were difference density peaks at the backbone atoms after refinement. Figure 3 shows the final model in a map computed with amplitudes ($|F_o| - |F_c|$) and phases derived from a round of refinement in which the atoms of residues 58 and 59 had been omitted from the calculated structure factors. Thus the data analysis leads us to conclude that the carbonyl group points away from the flavin (is O-down) in this crystal structure of reduced *A. nidulans* flavodoxin.

Reversion to the O-down conformation upon reduction to the hydroquinone was not predicted from studies of other flavodoxins. This rearrangement leads to changes in flavin protein interactions, relative to the semiquinone, and affects the interpretations of the sq/hq redox potentials that are presented in the Discussion.

Structures of the Asn58Gly mutant in the semiquinone and hydroquinone states

The Asn58Gly mutant crystallizes in form III, a cell with more open packing and higher solvent content (Drennan *et al.*, 1999), and the reduced states of the mutant in these crystals oxidize much more rapidly at 4°C than the reduced wild-type flavodoxins in crystal forms I or II. Data were

Table 4. Interactions of the isoalloxazine oxygen atom and nitrogen atoms

Structure/atom pair		Distances (Å)						
		N(1):90N	O(2):90N	O(2):99N	N(3):97O	O(4):60N	N(5):58O	N(5):59N
WT, ox	O-down	3.12	3.26	3.08	2.91	2.74		3.45
N58G, ox	O-down	3.13	3.32	3.05	2.92	2.76		3.70
D90N, ox	O-down	3.10	3.22	3.19	2.95	2.79		3.43
D100N, ox	O-down	3.10	3.22	3.19	3.05	2.74		3.46
WT, sq	O-up	3.06	3.24	3.06	2.94	2.86	2.81	
N58G, sq	O-up	2.99	3.15	3.06	2.95	2.80	2.85	
WT, hq	O-down	3.15	3.36	3.03	3.01	2.70		3.38
N58G, hq	O-up	3.07	3.18	3.02	3.01	2.80	2.97	

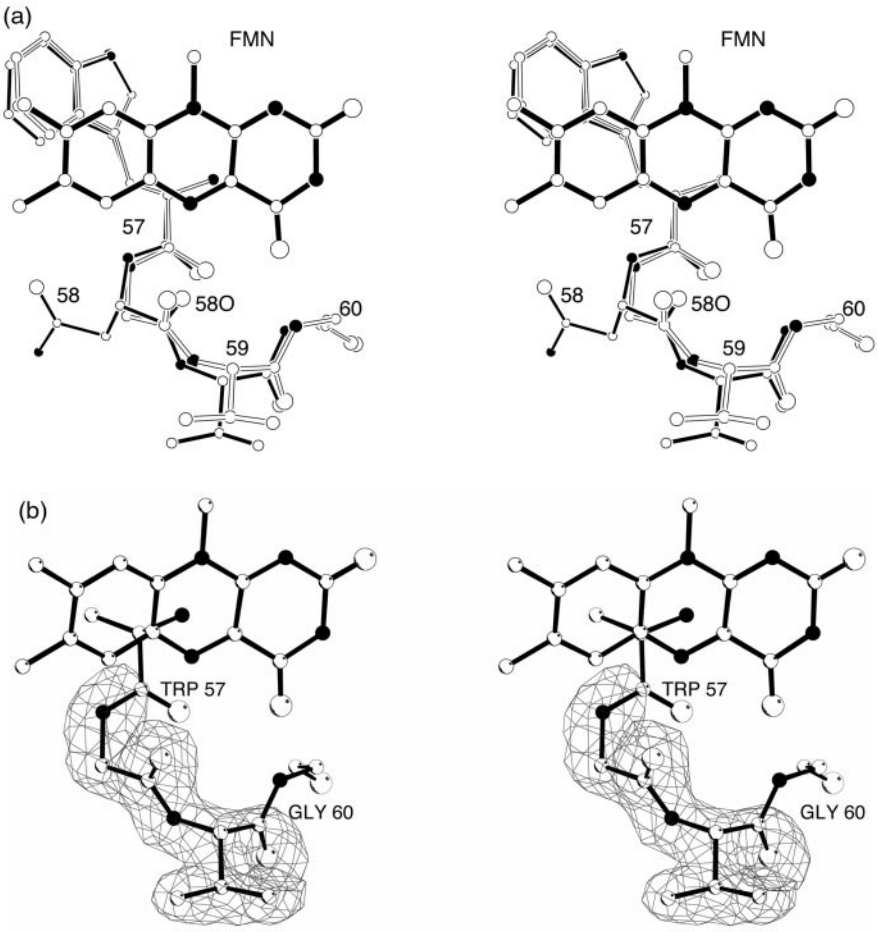

Figure 4. (a) A superposition of the conformations of residues 57-60 in the semiquinone forms of wild-type *A. nidulans* flavodoxin and the mutant Asn58Gly. The mutant is distinguished by the open bonds. (b) An ($|F_o| - |F_c|$) omit map of the hydroquinone form of the mutant Asn58Gly, contoured at 3σ. The Φ,Ψ angles at Asn58 and Val59 are (52, −133°) and (−117, 91°) in the hydroquinone structure (see Table 6).

therefore collected from crystals that had been reduced to the semiquinone or hydroquinone states and then frozen in the liquid nitrogen cooling stream (see Materials and Methods). The general strategy for structure determination was the same as for semiquinone and hydroquinone forms of wild-type flavodoxin. Protein coordinates from the oxidized form of the Asn58Gly mutant (Drennan *et al*., 1999) were first adjusted by rigid body refinement to compensate for the shrinkage in cell volume at 140 K. Further refinement in X-PLOR proceeded as described (Drennan *et al*., 1999). At the outset and in a final round of refinement, residues 58-59 were omitted to allow modelling and inspection of the density in this region of the structures.

After refinement *versus* data collected at 140 K (Table 2), the model for the semiquinone form of the Asn58Gly mutant included nearly twice as many solvent molecules as the structures based on measurements at 4 °C. Strong density modeled as a bound sulfate was observed near residue 35 and glycerol molecules were placed at two sites. In the final omit maps of the semiquinone form, the critical peptide at Gly58-Val59 is clearly O-up, with the carbonyl oxygen atom hydrogen bonded to N(5)H. As can be seen from Figure 4(a), the backbone conformations are nearly identical with those of wild-type *A. nidulans* in the semiquinone state.

The model for the hydroquinone form of the Asn58Gly mutant was similarly refined *versus* the 1.85 Å data collected at 140 K. Starting parameters for this oxidation state were from a partly refined model of the semiquinone form and were adjusted in an initial rigid body refinement. The absence of features in ($|F_o| - |F_c|$) difference maps implied that the 58-59 peptide in the fully reduced Asn58Gly mutant had retained the O-up conformation. Visual examination of the frozen crystal verified that it was pale yellow, consistent with presence of the FMN hydroquinone. The omit map shown in Figure 4(b) confirms that the 58-59 peptide is indeed O-up, in the same conformation as the semiquinone state (Figure 4(a)). Thus the hydroquinone form of the mutant adopts a structure that differs from wild-type: the Asn58-Val59 peptide does not revert to the O-down conformation.

We cannot exclude the possibility that crystal contacts may influence the equilibrium between up

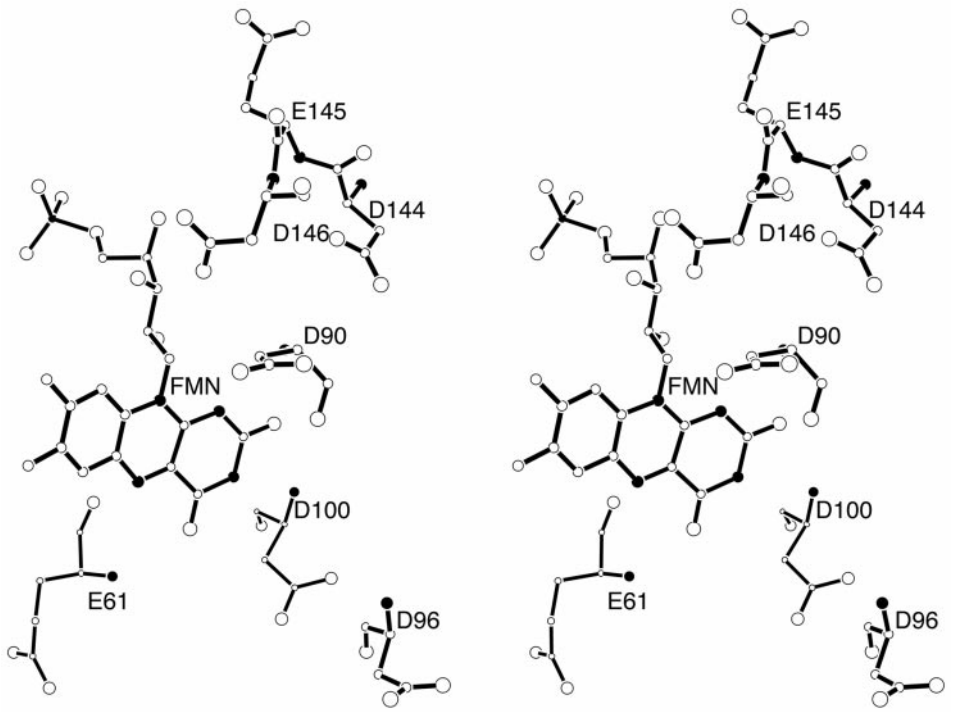

Figure 5. A stereodrawing showing the locations of residues Asp90 and Asp100, sites of mutation to Asn, along with other Asp and Glu residues in the vicinity of the isoalloxazine ring. Figure 3(b) by Drennan *et al*. (1999) shows the 90's loop and its relation to the flavin ring.

and down conformations of the loop (see Discussion). The intermolecular contacts that control crystal packing are described in the accompanying paper (Drennan *et al*., 1999). In the wild-type crystal forms I and II the side-chain of Asn58 packs against Tyr119 from a neighboring molecule, and the 58-59 region is involved in a number of additional contacts. In the form III crystals of the Asn58Gly mutant, the 50's loop is more exposed to solvent.

Structures of Asp90Asn and Asp100Asn flavodoxins

Aspartate residues at positions 90 and 100 lie in the connector between β4 and α3 that wraps around the flavin ring (Figure 5). Both residues are close enough to the flavin to affect the redox potentials *via* electrostatic interactions, even though they are partly accessible to solvent. Asp90 is conserved in all the long-chain flavodoxins, and in the known structures it interacts with the main-chain NH 93 in a helical turn (Drennan *et al*., 1999). Its carboxylate carbon atom is only 5.2 Å from the flavin N(1) and 6.2 Å from O(2); these atoms and O(4) carry a substantial fraction of the negative charge distributed on the hydroquinone anion (Hall *et al*., 1987c; Ludwig & Luschinsky, 1992; Zheng & Ornstein, 1996). Asp100 is found in most but not all long-chain flavodoxins; in *A. nidulans* flavodoxin it is the final residue of the type II turn that interacts with O(2) and N(3)H of the flavin ring. The carboxyl carbon atom of Asp100 is 6.8 Å from O(2) but separated from contact with the flavin ring by the intervening 97-98 peptide. The structures of the oxidized forms of the Asp90Asn and Asp100Asn mutants were determined by refinement starting from the type II form of the wild-type protein (Drennan *et al*., 1999), and are essentially the same as wild-type flavodoxin. The RMS deviations from wild-type for backbone atoms in the 89-99 loop are less than 0.4 Å for the mutants Asp90Asn and Asp100Asn. Since no detectable structural perturbations have been introduced by these mutations, the potential shifts can be attributed to changes in electrostatic interactions.

Redox potentials and association constants

Redox potentials were determined by titration or photoreduction in the presence of indicator dyes, and by potentiometry. The Nernst plots of data for the wild-type and mutant proteins are shown in Figure 6, and the midpoint potentials measured for wild-type, Asp90Asn, Asp100Asn, and Asn58Gly are listed and compared with previous measurements in Table 5. The mutations Asp90Asn and Asp100Asn have a relatively small effect on the ox/sq potentials, which increase by 15 and 10 mV, respectively. This suggests that electrostatic interactions play only a minor role in modulating the ox/sq equilibrium, which is not surprising since the net charge on the flavin does not change when oxidized FMN is reduced to the neutral semiquinone. Larger effects of the Asp90Asn and Asp100Asn mutations are seen in the sq/hq mid-

Table 5. Association constants (K_a) and oxidation-reduction potentials

Protein	Ox/sq (mV)	Sq/hq (mV)	$K_{a,\ FMNox}$	$K_{a,\ FMNsq}$	$K_{a,\ FMNhq}$
A. nidulans					
Wild-type	−221	−442	7.1×10^8	1.4×10^9	3.8×10^4
Asp90Asn	−206	−401	1.0×10^9	3.4×10^9	4.7×10^5
Asp100Asn	−210	−417	6.7×10^8	2.0×10^9	1.4×10^5
Asn58Gly	−175	−468	3.0×10^8	3.5×10^9	3.5×10^4
C. beijerinckii[a]					
Wild-type	−92	−399	5.5×10^7	1.7×10^{10}	2.4×10^6
Gly57Asn	−162	−372	1.7×10^7	3.3×10^8	1.4×10^5
Gly57Thr	−270	−320	3.1×10^7	9.1×10^6	2.8×10^4

All ox/sq midpoints have been adjusted to pH 7.0 assuming a slope of −59 mV/pH unit. The sq/hq midpoints for *A. nidulans* flavodoxin have not been adjusted for a redox-linked pK_a, which is observed at 6.1 in the flavodoxin from *Anabaena* 7119 (Pueyo *et al*., 1991). K_a for reduced states have been calculated from measured midpoint potentials.

[a] Potentials are from Mayhew *et al*. (1969) and Ludwig *et al*. (1997) and association constants from Chang & Swenson (1999).

point potentials, which increase by 41 mV and 25 mV relative to wild-type, as expected for elimination of charge repulsion between these residues and the anionic reduced flavin. The larger increase in the Asp90Asn mutant is consistent with its position closer to the negative N(1), O(2), and O(4) atoms of the flavin ring (see above). The observed shifts of the sq/hq potential are larger in magnitude than the average of 15 mV found in *D. vulgaris* mutants in which single Asp or Glu residues near FMN were replaced by Asn or Gln (Zhou & Swenson, 1995).

The mutation Asn58Gly raises the potential for the ox/sq equilibrium by 46 mV (−1.0 kcal/mol). This shift, which corresponds to stabilization of the semiquinone, is in the direction predicted by analysis of the conformational energies of the O-up and O-down forms (see Discussion), and is similar in magnitude to changes resulting from substitution of other residues for glycine in the 50's loop of *C. beijerinckii* flavodoxin (Ludwig *et al*., 1997). Substitution of glycine at position 58 also decreases the sq/hq potential, making full reduction more difficult.

The affinity of oxidized FMN for the apoproteins was determined from the quenching of FMN fluorescence that accompanies binding of FMN to flavodoxin. Apoprotein was added stepwise to standardized solutions of FMN and measurements were analyzed by fitting to the quadratic function that relates α, the fraction of flavodoxin present as holoprotein, to the total concentrations of protein and FMN (cf. Hoover & Ludwig, 1997; Lostao *et al*., 1997). Table 5 shows that the binding of oxidized FMN is not appreciably altered by the mutations Asp90Asn and Asp100Asn. The only deviation in binding affinity occurs in the case of the Asn58Gly mutant, which binds FMN more weakly than wild-type by a factor of about 2.5. Association constants of the order of 10^9 M^{-1}, which are characteristic for flavodoxins, are difficult to determine because very small concentrations of free FMN are present at equilibrium. Measurements of the affinity of *Anabaena* flavodoxin for oxidized FMN (Lostao *et al*., 1997) have determined a K_a of $\sim 3 \times 10^{10}$ M^{-1} ($\Delta G = -14.2$ kcal/mol), indicating even tighter binding than we have reported here for *A. nidulans* flavodoxin.

Binding constants for the semiquinone and reduced forms have been calculated from the K_a for oxidized FMN and the measured redox potentials, according to the thermodynamic cycles illustrated in Figure 1. An important property of *A. nidulans* flavodoxin, and of other long-chain flavodoxins that have low potentials for the two-electron reduction of oxidized FMN, is the decreased affinity of the protein for the hydroquinone form of the cofactor (Figure 1 and Table 5). Using the measured ΔG for binding of oxidized

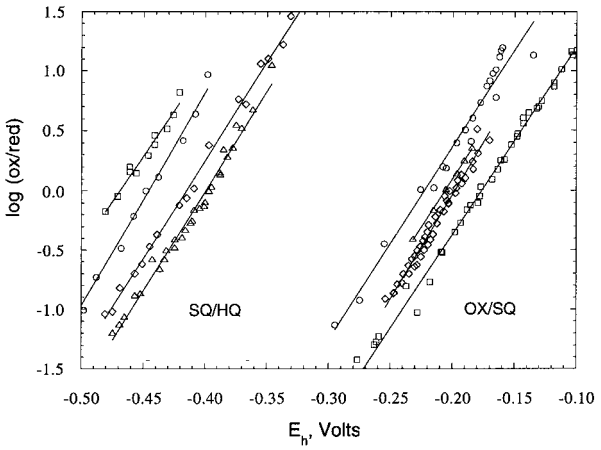

Figure 6. Nernst plots of the data from measurements of redox potentials. The ox/sq potentials (lines to the right) were all determined using xanthine/xanthine oxidase (XO) to generate reducing equivalents (Massey, 1991). The sq/hq potentials (left) were determined by several methods (see the text). Semiquinone/hydroquinone potentials for the mutants Asp90Asn and Asp100Asn were measured at pH 8.5 by the XO method, and taken to be the same at pH 7.0. The remaining sq/hq potentials were determined at pH 7.0 by photoreduction using dyes as indicators, and by potentiometric titration. Circles, wild-type; squares, Asn58Gly; triangles, Asp90Asn; diamonds, Asp100Asn.

FMN to *A. nidulans* flavodoxin (−12.1 kcal/mol), the calculated ΔG for binding of FMN hydroquinone is only −6.5 kcal/mol, corresponding to a K_a of 4×10^4 M^{-1}. With binding constants in this range, reduced FMN may dissociate from the protein. However, if equilibrium constants for binding of oxidized FMN to long-chain flavodoxins were actually closer to 10^{10} M^{-1} as found for *Anabaena* flavodoxin, then the calculated affinity for the hydroquinone would increase correspondingly and loss of reduced FMN would be minimized.

Discussion

In these studies we have asked how a long-chain flavodoxin modulates the redox potentials of bound FMN. For the short-chain flavodoxins from *C. beijerinckii* and *D. vulgaris*, conformation changes and the interactions of N(5)H with the protein are important determinants of the ox/sq equilibrium (Ludwig *et al*., 1997; O'Farrell *et al*., 1998; Watt *et al*., 1991), whereas charge effects appear to dominate the energetics for the sq/hq equilibrium (Zhou & Swenson, 1995). We have compared the structures of the oxidized, semiquinone, and hydroquinone states of *A. nidulans* flavodoxin to define conformation changes and alterations in FMN-protein interactions that occur when FMN is reduced. Site mutations have provided tests that allow estimates of the magnitudes of some of the energy contributions. Finally, special features of redox control in long-chain flavodoxins have been revealed by contrasts with the properties of *C. beijerinckii* flavodoxin.

The extent to which an apoprotein perturbs the redox potential of FMN is linked to differences in binding affinity as shown in the thermodynamic cycles of Figure 1. The equilibrium binding constants, K_a, might be expected to vary with flavin oxidation state, even in the absence of any changes in the protein, because reduction alters the electronic properties of the flavin ring (Hall *et al*., 1987c). Addition of H^+ and e^- to form the semiquinone redistributes charge and creates a hydrogen bond donor at N(5); in flavodoxins, addition of the second electron at pH 7 or above forms the hydroquinone anion, with a net −1 charge on the isoalloxazine ring. Thus non-covalent interactions between the protein and the isoalloxazine ring will differ in energy as the flavin is reduced.

Rearrangements of the protein that accompany reduction can magnify the influence of the protein on potentials. Conformation changes have two consequences, each of which can significantly affect redox equilibria: they may generate or eliminate protein-FMN interactions; and the energy associated with any conformation change is a part of the total energy required for reduction. Recent structure-function analyses of *C. beijerinckii* flavodoxin and several mutants (Ludwig *et al*., 1997) have shown that the change in conformational energy associated with the peptide flip to O-up can make a substantial contribution to the ox/sq potential. In those analyses it was convenient to separate the contributions of the protein to potential shifts into two components, ΔG_c arising from changes in the protein structure that accompany reduction, and $\delta\Delta G_i$, from the differences in flavin-protein interaction energy that accompany reduction. A similar scheme is followed here, and is shown in Figure 7. This scheme focuses on perturbations in conformation and perturbations of interactions that occur when the bound FMN is reduced to the semiquinone or hydroquinone forms and does not attempt to account for the overall energy of binding (cf. Lostao *et al*., 1997).

The ox/sq potential in *A. nidulans* flavodoxin

Hydrogen-bonding at N(5) and conformation changes

The formation of the semiquinone species in *A. nidulans* flavodoxin is accompanied by a peptide rearrangement that allows a carbonyl oxygen atom to hydrogen bond to the N(H)5 position of the flavin ring. Resulting differences in flavin-protein interactions that can be discerned by comparing structures of the oxidized and semiquinone forms include formation of the O58-N(5)H hydrogen bond in the semiquinone structure, loss of the NH

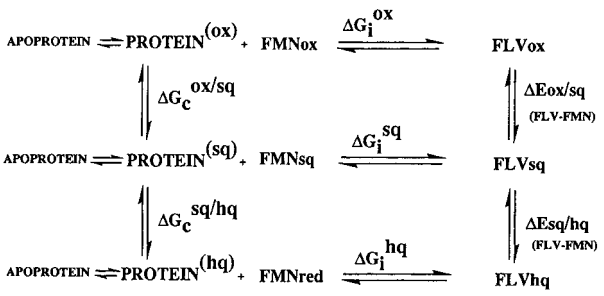

Figure 7. A thermodynamic scheme for analysis of energetic contributions to redox potential shifts. This scheme describes how free energies of FMN reduction are perturbed when FMN is bound to flavodoxin. Apoprotein (far left) is in equilibrium with PROTEIN$^{(i)}$, a hypothetical apoprotein species which has the conformation characteristic for the oxidized, semiquinone, or hydroquinone state of the holoprotein. ΔG_c (vertical equilibria on the left) are the energy differences between the PROTEIN$^{(i)}$ structures. ΔG_i (horizontal equilibria on the right) are free energy changes associated with the interaction of FMN (ox, sq, or hq) with the corresponding apoprotein (PROTEIN$^{(ox)}$ interacts with FMNox, etc.). ΔG_i is not the same as the measured binding free energies, which are for reaction of FMN with APOPROTEIN. ΔE, in the right-hand vertical limbs, are the measured shifts in potential, relative to free FMN. ΔE values must equal the sum of the steps around each box, e.g. $\Delta E(\text{ox/sq}) = \Delta G_c^{ox/sq} + \Delta G_i^{sq} - \Delta G_i^{ox}$. In this example, $\delta\Delta G_i = \Delta G_i^{sq} - \Delta G_i^{ox}$, the change in protein-flavin interaction energies accompanying reduction to the semiquinone. (Reproduced from Ludwig *et al*. (1997) with permission.)

Table 6. Dihedral angles in the 50's loops of *A. nidulans* flavodoxins

Oxidation state	$(\Phi,\Psi)_2$	$(\Phi,\Psi)_3$	$(\Phi,\Psi)_4$
Oxidized, wild-type	45, 50	58, 70	88, 13
Oxidized, Asn58Gly	45, 35	59, 74	87, 22
Semiquinone, wild-type	53, -131	−101, 84	59, 44
Semiquinone, Asn58Gly	56, -130	−122, 94	62, 38
Hydroquinone, wild-type	42, 48	66, 77	70, 28
Hydroquinone, Asn58Gly	52, -133	−117, 91	64, 39

These are the central residues, [58]Asn-Val-Gly, of the three-residue turn.

59 to N(5) contact that is found in the oxidized structure, and introduction of an approximately parallel dipole-dipole interaction between C-O 58 and C-O(4) of flavin in the O-up semiquinone conformation. These are important contributors to the change in interaction energy that accompanies reduction, called $\delta\Delta G_i$ (see Figure 7). Comparing the hydrogen bond at N(5)-HN 59 in the oxidized structure with the hydrogen bond at O 58-N(5)H in the semiquinone form suggests that O 58-N(5)H is the stronger of the two bonds. The N(5)-HN 59 distance in the oxidized structure is relatively long, 3.4 Å or greater (Table 4). At the same time, the high pK_a of N(5)H in the semiquinone of *A. nidulans* flavodoxin implies that the N(5)H-O 58 hydrogen bond is strong†. The N(5)H pK_a increases from 8.5 in free FMN semiquinone to ~13.1 in the protein (D.M.H. & D.B. Ballou, unpublished observations). Replacement of the N(5)-HN 59 interaction in the oxidized flavodoxin by the N(5)H-O 58 bond in the semiquinone state therefore appears energetically favorable. This favorable exchange of hydrogen-bonding interactions is countered by the repulsive dipole interactions between CO 58 and C(4)-O(4) in the O-up conformation.

The O-up and O-down arrangements also differ in conformational energy (ΔG_c). ΔG_c is not accessible to experiment but may be examined by computation. One simple approach is to compare energies for the conformations of individual residues in the oxidized and semiquinone structures (Table 6). The Ramachandran angles (Ramachandran & Sasisekharan, 1968) for residue 58 in oxidized flavodoxin are $\Phi = 44$, $\Psi = 54$ (α_L) and change to $\Phi = 53$, $\Psi = -131$ in the semiquinone state. The latter angles are characteristic for the second position of a type II′ turn, and are rarely observed for residues other than glycine (Hutchinson & Thornton, 1994; Richardson, 1981). With non-glycine residues this conformation has high energy because of very close contacts between the C^β atom and the following NH group; in *A. nidulans* flavodoxin the contact is between the C^β atom of Asn58 and the nitrogen atom of Val59. From energy landscapes calculated for the alanine dipeptide in the presence of solvent (Anderson & Hermans, 1988) the difference between the oxidized and semiquinone conformers of Asn58 may be estimated as 1.5-2.0 kcal/mol, with the oxidized conformation having lower energy. This cost of semiquinone formation, incurred by unfavorable geometry at position 58, may be more than compensated by changes at Val59 which take this residue from a left-handed alpha conformation in oxidized flavodoxin to the more favorable β-region in the semiquinone state (Table 6). The conformation of Val59 in the semiquinone structure is favored by 2.0-2.5 kcal/mol (Anderson & Hermans, 1988). Use of statistical Φ,Ψ distributions for individual residues could provide additional estimates (Hutchinson & Thornton, 1994; Munoz & Serrano, 1994). Free energy perturbation calculations (Scully & Hermans, 1994) for our particular structures may offer a better way to calculate ΔG_c.

Analysis of the changes in interaction and conformation and how they affect potentials is formalized in Figure 7. Ways in which the protein can affect the ox/sq equilibrium of FMN are shown in the upper thermodynamic cycle of the Figure. The conformation change contributes an energy ΔG_c; differences between flavin-protein interactions in the semiquinone and oxidized states, $\delta\Delta G_i$, also contribute to the resultant potential shift, ΔE. In *A. nidulans* flavodoxin, the ox/sq potential is almost identical with that measured for free FMN by Draper & Ingraham (1968). For the shift in potential, ΔE (protein *versus* free FMN), to be zero, the change in conformational energy, ΔG_c, must be matched by the differences in interaction energies between the oxidized and semiquinone states.

The Asn58Gly mutant

Replacement of Asn58 by a glycine residue provides an experimental test of the prediction that the semiquinone lower loop conformation is destabilized by the presence of Asn at position 58. The X-ray analysis of the semiquinone form of the mutant verifies that Gly 58 is O-up although the conformation of the loop differs somewhat from wild-type, particularly at Val59 (Figure 4(a)). The effect of replacing Asn with Gly at position 58 in the semiquinone can be estimated from relative energies for II′ turns with Ala or Gly as −1.3 kcal/mol (Yang *et al*., 1996). Comparisons of Ramachan-

† The pK_a values for N(5)H in several flavodoxin semiquinones have been measured in pH jump experiments (Ludwig *et al*., 1990, 1997). In the flavodoxin from *C. beijerinckii*, the pK_a of the semiquinone N(5)H is too high to be measured and must be greater than 13.5.

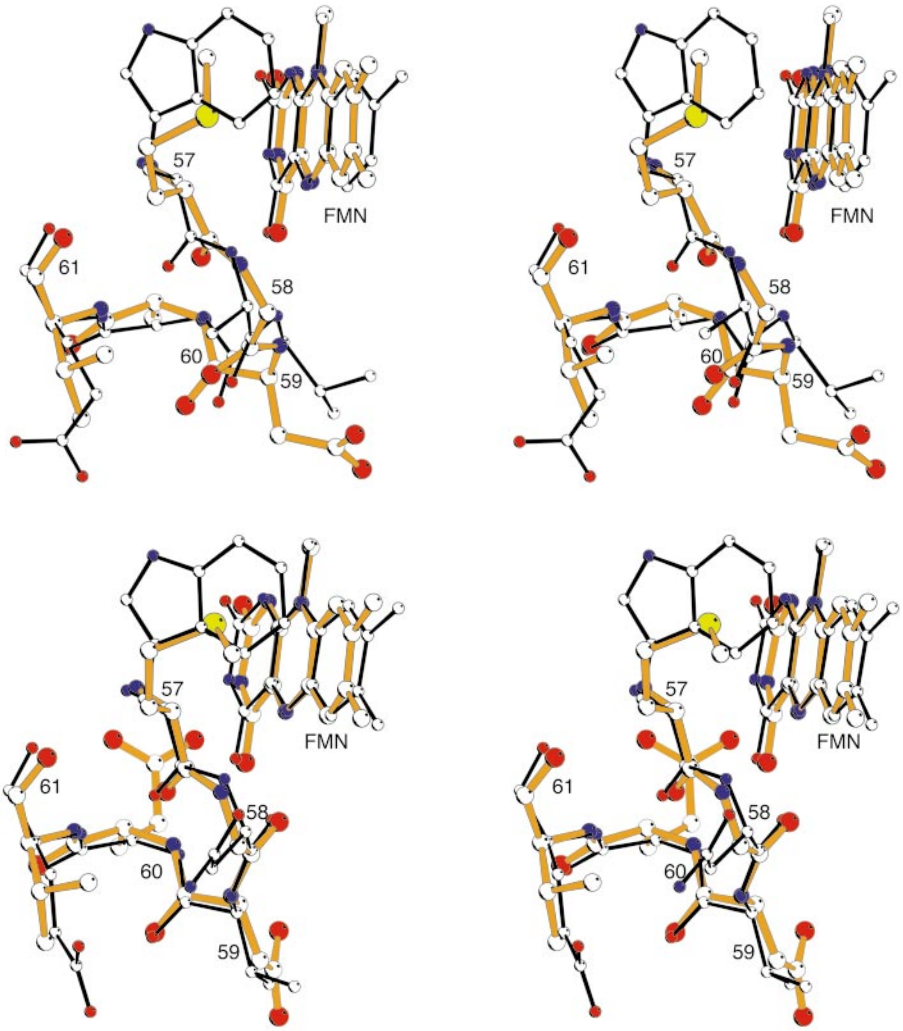

Figure 8. (a) A local comparison of oxidized *A. nidulans* flavodoxin and the *trans* O-down conformer of *C. beijerinckii* flavodoxin. The model for *C. beijerinckii* flavodoxin is drawn with thick gold bonds and the model for *A nidulans* flavodoxin with thinner black bonds; oxygen atoms are red, nitrogen atoms are blue, and carbon atoms are white. The greater distance from N(5) to the 57-58 backbone, and the unfavorable N–H–N angle, preclude hydrogen bonding between N(5) and NH 58 in *C. beijerinckii* flavodoxin. The structures were aligned by matching atoms of the flavin rings and the five C^{α} atoms of the loops. To simplify the drawing, side-chains Asn58 (*A. nidulans*) and Glu59 (*C. beijerinckii*) have been truncated. (b) A local comparison of the semiquinone forms of flavodoxins from *C. beijerinckii* and *A. nidulans*. Structures were aligned as in (a). Residue numbers are for *A. nidulans* flavodoxin.

dran maps for Ala and Gly peptides suggest a larger difference, about −3 kcal/mol. These estimates correspond to an increase in ox/sq potential of 60 to ~135 mV. The measured potential of the Asn58Gly mutant is 46 mV more positive than wild-type, and shows the expected effect of relieving close contacts within the flipped peptide, although the observed change is smaller in magnitude than predicted from the estimates of conformational energies.

Comparisons with C. beijerinckii flavodoxin

The analyses of *A. nidulans* flavodoxin confirm that N(5)H interactions with the lower loop are a general mechanism used by flavodoxins to stabilize the semiquinone state. Reduction of wild-type *A. nidulans* flavodoxin to the semiquinone leads to an O-up conformation that is locally very similar to that found in the semiquinone of *C. beijerinckii* flavodoxin. The isoalloxazine-protein geometries in *C. beijerinckii* and *A. nidulans* flavodoxins are compared in Figure 8. In both species a conformation change is required to generate a favorable protein-N(5)H interaction. However the ox/sq potential of *C. beijerinckii* flavodoxin (with a Gly-Asp peptide) is about 130 mV higher (Table 1), making reduction of clostridial flavodoxin much more favorable. One key difference between the species is the presence of Asn58 in *A. nidulans* flavodoxin, which raises the energy of the O-up semiquinone conformer. Substitution of Gly for Asn favors

reduction (Table 5), increasing the potential by 46 mV (−1.0 kcal/mol) in *A. nidulans* flavodoxin, and by 70 mV (−1.5 kcal/mol) in *C. beijerinckii* flavodoxin (Ludwig *et al*., 1997). In addition, the structures of the loops in the two oxidized flavodoxins are not alike. A unique feature of oxidized *C. beijerinckii* flavodoxin is the presence of a mixture of conformers, including a fraction of *cis* peptide, at the critical 57-58 positions (Ludwig *et al*., 1997). By comparison with a Gly57-Pro58 mutant that is *cis* O-down in oxidized flavodoxin and *trans* O-up in the semiquinone, the shift in ox/sq potential that results from the presence of this particular mixture of conformers has been estimated as ∼60 mV (−1.4 kcal/mol). The measured effects on ΔG_c of substituting Gly for Asn at the flip position (45-70 mV), combined with the contribution from the *cis* peptide, predict an increase in potential of 105-130 mV for *C. beijerinckii* flavodoxin relative to *A. nidulans* flavodoxin. Together these contributions would account for much of the 130 mV difference in ox/sq potential between the two flavodoxins.

The N(5)-HN 59 interaction, discussed by Drennan *et al*., (1999), is a special structural feature found in oxidized flavodoxins from *A. nidulans*, *Anabaena* (Burkhart *et al*., 1995) and *E. coli* (Hoover & Ludwig, 1997). Rao *et al*. (1992) have proposed that these N(5)-HN 59 contacts found in several long-chain flavodoxins are functionally significant features that act to lower ox/sq potentials by stabilizing the oxidized structure†. According to the calculations by Hall *et al*. (1987c), the N(5) of oxidized flavin has an atomic charge of -0.01, and therefore would be a relatively poor hydrogen bond acceptor. However more recent computations (Zheng & Ornstein, 1996) assign a much more negative charge (−0.518) to N(5). NMR measurements on flavodoxins from *Anabaena* 7120 (Stockman *et al*., 1988) and *A. nidulans* (Clubb *et al*., 1991) are consistent with hydrogen bonding; the N(5) chemical shifts in the oxidized ^{15}N-labelled proteins are very close to the shift for free FMN in water and differ from the shifts in apolar solvents. Thus despite the rather long donor-acceptor distances of 3.0 to 3.6 Å this characteristic N(5)-HN 59 contact appears to play a role in the energetics of long-chain flavodoxins. A comparable interaction is not possible in oxidized *C. beijerinckii* flavodoxin, even in a *trans* O-down conformer, because the N(5)-HN 58 distance of 4.1 Å is too long and the N−H−N angle is unfavorable.

The sq/hq potential in *A. nidulans* flavodoxin

Effects of charge and flavin environment

Attention has focused on electrostatic repulsion as the basis of the low sq/hq potentials and the weak binding of the anionic flavin hydroquinone by the short-chain flavodoxins from *C. beijerinckii* and *D. vulgaris*. In the framework shown in Figure 7, unfavorable FMN-protein interactions (ΔG_i) in the hydroquinone state appear to dominate the thermodynamics of the lower cycle that describes the sq/hq equilibrium. Recent studies of *D. vulgaris* flavodoxin (Zhou & Swenson, 1995, 1996a) have directly demonstrated the importance of electrostatic repulsion in lowering the sq/hq potential; replacements of acidic residues near the flavin ring increase the sq/hq potential, with an increment that depends on location but averages about 15 mV per residue. Measurements of the redox potentials of riboflavin bound to *D. vulgaris* flavodoxin suggested that the FMN phosphate also contributes to charge repulsion (Curley *et al*., 1991), but examination of mutants indicates that interactions with phosphate charges do not dominate the sq/hq potential (Zhou & Swenson, 1996b).

An examination of the flavin binding site in *A. nidulans* flavodoxin shows seven acidic residues located within 15 Å of the flavin N(1) without any compensating positive charges (Figure 5). These negatively charged aspartate and glutamate residues are expected to generate repulsive electrostatic interactions when the neutral semiquinone is reduced to the flavin hydroquinone, which is assumed to be the anion by analogy with *Anabaena* flavodoxin (Stockman *et al*., 1988). Magnitudes of each of the interactions are dependent on distance and screening (Honig & Nicholls, 1995), and on the distribution of charge in the bound reduced flavin. As reported here, increases in the sq/hq potential of 25 mV and 41 mV, larger than the average effects of single mutations in *D. vulgaris* flavodoxin, result from the substitutions Asp100Asn and Asp90Asn, respectively. Thus electrostatic effects in flavodoxin hydroquinones provide a general mechanism for lowering potentials that seems to be shared by all flavodoxins. A cluster of negatively charged residues that occurs near position 145 in all long-chain flavodoxins (Figure 5) may be important in maintaining the low sq/hq potentials of these proteins.

A. nidulans and *D. vulgaris* flavodoxins have lower sq/hq potentials than *C. beijerinckii* flavodoxin (see Table 1). Relative solvent accessibility of the flavin may be one reason. The low molecular mass flavodoxins from *C. beijerinckii* and *M. elsdenii* have short sequences in the 90's region that follows β4 and contacts the flavin. In these flavodoxins the side-chain of Glu59 interacts with N(3)H of the flavin ring, in place of backbone atoms from the 90's loop (see Figure 3(b) in the paper by Drennan *et al*., 1999). These features of *C. beijerinckii* flavodoxin leave a channel for solvents at the pyrimidine end of the flavin ring. In *D. vulgaris* and *A. nidulans* flavodoxins, three to five residues are inserted in the 90's region, and a backbone C-O from this region hydrogen bonds to N(3)H. The additional residues wrap around the flavin and block access of solvent, creating a more apolar environment which should disfavor the formation of the anionic flavin.

† In the long-chain flavodoxin from *C. crispus* (Fukuyama 1992), the side-chain of Thr58 interacts with N(5). See Figure 5 in the paper by Drennan *et al*. (1999).

Mutations of the aromatic residue that stacks over the flavin ring have demonstrated the importance of solvent accessibility. Swenson & Krey (1994) substituted several amino acid residues for Tyr98 of *D. vulgaris* flavodoxin, which is equivalent to Tyr94 in *A. nidulans* flavodoxin. The mutation Tyr98Ala opens the flavin ring to solvent and raises the sq/hq midpoint potential by 140 mV; the corresponding mutation in *Anabaena* flavodoxin increases the sq/hq potential by 137 mV (Lostao *et al*., 1997).

A conformation change at Asn58-Val59 affects the sq/hq potential?

Finding the 58-59 peptide in the O-down conformation in wild-type *A. nidulans* flavodoxin hydroquinone was unexpected. Does this ''back-flip'' also occur in solution or is it promoted by contacts and conditions in the crystal? To examine intermolecular interactions in crystal form I with the 58-59 peptide in the O-up conformation, we superimposed the O-up conformer on the model for oxidized form I flavodoxin. There are no intermolecular hydrogen bonds that favor O-down over O-up in these crystals. However the backbone C-O dipole of Asn58 and the O-H dipole of Tyr119 of the neighbor molecule are separated by 4.8 Å in a favorable antiparallel arrangement in the O-down hydroquinone structure, but are parallel and less than 5 Å apart in the model of the O-up conformation. Mutation of Tyr119 might ascertain whether this intermolecular interaction is critical in determining the conformation of residues 58-59. The hydroquinone form of the Asn58Gly mutant adopts the O-up loop structure in its different and less closely packed crystal form. This finding does not prove that intermolecular interactions in crystal form I force the wild-type hydroquinone into the O-down conformation, since the O-up conformer is intrinsically more stable in the glycine mutant than in the wild-type protein, as discussed above. The differences between the wild-type and Asn58Gly structures do suggest that the equilibrium between O-up and O-down in the reduced flavodoxin, which depends on both conformational and interaction energies, is rather delicately balanced in fully reduced *A. nidulans* flavodoxin.

NMR measurements on the hydroquinone form of the closely related flavodoxin from *Anabaena* (Stockman *et al*., 1988) show chemical shifts of ^{15}N(5) that are upfield from those in the hydroquinone forms of *C. beijerinckii* or *D. vulgaris* flavodoxins, suggesting weak hydrogen bonding of N(5)H (Vervoort *et al*., 1986) in *Anabaena* flavodoxin. In crystal structures of both short-chain flavodoxin hydroquinones the backbone carbonyl group is clearly in the O-up conformation and hydrogen bonded to N(5)H. The apparently weaker hydrogen bonding of N(5)H in *Anabaena* flavodoxin might be consistent with an O-down conformation of Asn58. However, further experiments will be required to assign unambiguously the loop conformation in the hydroquinone forms of *Anabaena* or *A. nidulans* flavodoxins. More detailed NMR analyses of the solution conformation and crystal structures of mutants that alter intermolecular interactions would both be helpful.

If Asn58-Val59 reverts to the O-down arrangement in the hydroquinone state in solution, then the energetics of the sq/hq equilibrium (represented in the lower thermodynamic box shown in Figure 7) must include contributions from a conformation change (ΔG_c) and from the resulting alterations in flavin-protein interactions. ΔG_c for the sq/hq equilibrium will be opposite in sign to ΔG_c in the cycle that determines the ox/sq potential. Energies associated with FMN-loop contacts in the O-down form will not be identical in the hydroquinone and oxidized states even though the loop atoms are in the same positions. For example, N(5)-HN 59 hydrogen bonding appears to stabilize the oxidized form, whereas the N(5)H-HN 59 contact in the hydroquinone is presumably unfavorable, and the O(4)-HN 60 hydrogen bond will be significantly stronger in reduced flavodoxin because of the larger charge on O(4) (Hall *et al*., 1987c) Although the altered contacts between loop atoms and the N(5) edge of the flavin would contribute to $\delta\Delta G_i$ for the sq/hq equilibrium, charge repulsions between the buried hydroquinone anion and protein carboxylate groups are likely to dominate ΔG_i^{hq} (Figure 7) whether the hydroquinone loop conformation is up or down.

Why does the sq/hq potential decrease in the Asn58Gly mutant?

The Asn58Gly mutation in *A. nidulans* flavodoxin raises the ox/sq potential but lowers the sq/hq potential. These effects parallel previous observations from studies of *C. beijerinckii* (Ludwig *et al*., 1997) and *D. vulgaris* (Mayhew *et al*., 1996) flavodoxins, in which mutations in the lower loop region shift the ox/sq and sq/hq potentials in opposite directions. Mutations of the loop residues appear to destabilize or stabilize the semiquinone without much perturbation of the free energy for the overall two-electron reduction of the protein bound FMN. Another way to describe this trend is to say that it is easier to add a second electron to a flavodoxin semiquinone that has been destabilized by mutation. We have considered previously the rationalization that the energies of loop-FMN interactions are large in the semiquinone, making stabilization of the semiquinone particularly sensitive to changes in structure and sequence of the critical loop (Ludwig *et al*., 1997).

It is reasonable for interactions involving the N(5) edge of the flavin ring to affect potentials, since the LUMO in oxidized flavin that resembles the HOMO in the hydroquinone is centered on N(5)-C(4a) (Hall *et al*., 1987a). The spin density distribution calculated for isoalloxazine semiquinones is particularly sensitive to protonation of N(5) (Zheng & Ornstein, 1996) . A mutation that affects

hydrogen bonding of the O-up conformer to N(5)H may thus alter the electronic energy of the semiquinone by perturbing the spin density distribution: one expects a correlation between potentials and hydrogen-bond strength. Consistent with this idea is the observation that the pK_a of N(5)H in the destabilized semiquinone of the *C. beijerinckii* mutant G57T ($E_{ox/sq} = -270$ mV) is only 11.5, much lower than the pK_a of wild-type (Ludwig *et al*., 1997). Very recent measurements estimating the strengths of the N(5)H hydrogen bond in the hydroquinone forms of *C. beijerinckii* flavodoxin and several mutants demonstrate a positive correlation between the strength of the hydrogen bond to N(5)H and the ease of formation of the semiquinone, as measured by the ox/sq potential (Chang & Swenson, 1999).

Redox control in *A. nidulans* and related long-chain flavodoxins

Conformation changes play an important role in determining the ox/sq potentials in *A. nidulans* flavodoxin, just as they do in *C. beijerinckii* flavodoxin (Ludwig *et al*., 1997). The peptide flip at Asn58-Val59 offers a hydrogen bond acceptor to N(5)H in the semiquinone state and contributes *per se* to the free energy change associated with reduction. In addition, the conformational switch in *A. nidulans* flavodoxin and its close relatives also allows an N(5) to backbone NH interaction to stabilize the oxidized structure.

Magnitudes of the conformational energy contributions are sensitive to the sequence of the 50's loop, as demonstrated by studies of the Asn58Gly mutant of *A. nidulans* flavodoxin. We surmise that contributions from conformational energies are very similar in *A. nidulans* and *Anabaena* flavodoxins, since the loop sequence ^{57}Trp-Asn-Val-Gly-Glu in *A. nidulans* is altered in *Anabaena* flavodoxin only by substitution of Ile59 for Val. It remains to be shown whether *E. coli* flavodoxin, in which Asn-Val is replaced by Tyr-Tyr, adopts the O 58-up conformation in the semiquinone or hydroquinone states. In the short-chain *D. vulgaris* (Watt *et al*., 1991) and *D. desulfuricans* (Romero *et al*., 1996) flavodoxins, conformation changes also contribute to redox behavior, but the structures and structural changes differ from those in *C. beijerinckii* or *A. nidulans* flavodoxins.

The data obtained from studies in several laboratories (Lostao *et al*., 1997; Ludwig *et al*., 1997; Zhou & Swenson, 1995) indicate that unfavorable electrostatic interactions of the reduced flavin anion, which is mostly buried and inaccessible to solvent, are responsible for the uniformly low sq/hq potentials of flavodoxins. These electrostatic effects may also dominate the overall two-electron midpoint potentials, which are all lower than in free FMN and are generally lower in long-chain than in short-chain flavodoxins (Table 1).

Some distinctive properties of the long-chain flavodoxins from *A. nidulans*, *E. coli*, and *Anabaena* emerge from this work and from earlier studies. First, the longer 90's loops of long-chain flavodoxins restrict solvent access to FMN and act to enhance electrostatic effects. The apolar environment, and the distribution of Asp and Glu residues in long-chain flavodoxins, serve to lower the potential for overall two-electron reduction of oxidized flavodoxin. Second, as initially suggested by Rao *et al*. (1992), the N(5)-backbone NH interaction in the oxidized forms stabilizes that state, making reduction less favorable. Finally, as the current analysis of reduced and mutant *A. nidulans* flavodoxins shows, H-bonding of N(5)H in the semiquinone and reduced forms is weaker than in some of the short-chain flavodoxins. This conclusion is supported by the pK_a of N(5)H in the semiquinone and especially by the tendency of the 58-59 peptide to revert to the O-down conformation in the hydroquinone state. The overall consequence of somewhat stronger hydrogen bonding in the oxidized structure and weaker hydrogen bonding in the reduced forms is to shift potentials downward. Thus our studies of *A. nidulans* flavodoxin further emphasize the general importance of protein interactions with N(5) and with N(5)H for control of redox potentials. Direct measurements of the strengths of these isoalloxazine-protein hydrogen bonds in several flavodoxins would be very informative, and further investigation of electrostatic contributions in other long chain flavodoxins is clearly warranted.

Materials and Methods

Construction of mutants and purification of flavodoxin from overexpressing strains

Site mutants were generated using a commercial *in vitro* mutagenesis system (Amersham) based on the method by Eckstein (Olsen *et al*., 1993; Sayers *et al*., 1988), with mutagenic oligonucleotides designed to produce specific amino acid substitutions. The single-stranded DNA template used in this system was derived from Bluescript plasmids (Stratagene) carrying the *A. nidulans* flavodoxin gene. The plasmid construction, expression, and purification of the wild-type flavodoxin have been described (Clubb *et al*., 1991).

Reduction of crystals

Reduced forms of both wild-type and the mutant Asn58Gly were obtained by dithionite reduction of pregrown crystals (Correll, 1992). For conversion to the semiquinone, dithionite (5-10 mM) was dissolved in holding solution (2.6 M ammonium sulfate, 150 mM KP_i (pH 6.8)) that had been made anaerobic by evacuation and flushing with argon. The crystal, in holding solution in a melting point capillary, was transferred into a glove box and resuspended several times in the dithionite solution until it became dark blue-black. It was then transferred by inverting the melting point tube into an X-ray capillary filled with anaerobic holding solution. The mount was completed as usual and the X-ray capillary was sealed using epoxy. To obtain hydroquinone species, the pH was adjusted to 8.5 by replacing the buf-

fer with 150 mM Tris-HCl (pH 8.5), and the dithionite concentration was increased to 35 mM. The hydroquinone state could be distinguished from the semiquinone state by inspection; crystals of the hydroquinone form are bleached and appear pale green or yellow depending on orientation.

Data for refinement of the semiquinone and hydroquinone forms of the Asn58Gly mutant were collected from crystals that had been flash-frozen. Reduction of the crystals was performed as above, except that 15% (v/v) glycerol was included in the holding solution and the ammonium sulfate concentration was raised to 3.0 M. After a crystal was reduced to either the semiquinone or hydroquinone state, the melting point tube with the crystal was removed from the glove box, and the crystal was decanted onto a small Kevlar loop, fastened atop a metal pin by epoxy. The crystal was flash frozen under a stream of cold nitrogen gas (90-100 K) within 30 seconds, or instantly plunged into liquid nitrogen. The temperature of the freezing stream was raised to 140 K for data collection.

Data collection and refinement

Crystallizations of three different forms of *A. nidulans* flavodoxin have been described by Drennan *et al*. (1999). The forms used in each experiment are indicated in Tables 2 and 3. Data sets were collected with an ADSC dual area detector system using a Rigaku RU200 rotating anode X-ray generator as the X-ray source. The beam emerging from a graphite monochromator (Supper) was collimated to a diameter of 0.5 mm. The data collection strategy was as described for an orthorhombic crystal (Xuong *et al*., 1985). A typical step size was 0.12 deg., and detector-crystal distances were 555 and 612 mm. The data were collected and processed using the San Diego software package (Howard *et al*., 1985). Experiments at low temperature employed an Enraf-Nonius cryocontroller and transfer system.

Refinements were carried out with the algorithms in X-PLOR (Brünger, 1992; Brünger *et al*., 1990) as described in the accompanying paper. See Table 3 for the refinement statistics.

Protein Data Bank accession numbers

The coordinates have been deposited in the Protein Data Bank with PDB accession codes 1CZL (wild-type semiquinone), 1D04 (wild-type hydroquinone), 1CZH (Asn58Gly semiquinone), 1CZO (Asn58Gly hydroquinone), 1CZR (oxidized Asp90Asn), and 1CZK (oxidized Asp100Asn).

Measurement of redox potentials

The primary method for measurement of ox/sq potentials used xanthine and xanthine oxidase to generate reducing equivalents, with dyes as mediators and indicators (Massey, 1991). Flavodoxin was mixed with buffer, an indicator dye (either anthraquinone-2-sulfonate, AQ2S, or anthraquinone-2,6-disulfonate, AQ2,6DS), mediator (methyl viologen, MV), and xanthine in a cuvette designed for anaerobic titrations. The buffer was 100 mM phosphate (pH 7.0), except where noted otherwise. Xanthine oxidase was placed in the sidearm, and the cuvette was closed and made anaerobic with 10-15 cycles of evacuation and flushing with argon. Xanthine oxidase was introduced and mixed, and spectra were recorded with a diode array detector every two to ten minutes, depending on the amount of xanthine and xanthine oxidase present. Concentrations of oxidized and semiquinone flavodoxin, and of oxidized and reduced indicator dye, were calculated from the visible absorbance spectra.

To measure the sq/hq potentials of flavodoxin with xanthine/xanthine oxidase, the pH was raised to 8.5 (100 mM Tris) where xanthine is a better reductant. The sq/hq potentials of flavodoxin are independent of pH in the range 7.0 to 9.0, whereas the xanthine/urate couple is pH dependent with $E_m = -440$ mV at pH 8.5 (Massey, 1991). Protocols were the same as for measurement of the ox/sq potentials, except that MV was used as both mediator and indicator. Because there are no discernable isosbestic points in the sq/hq spectral transition, the spectrum of reduced MV was subtracted manually from the measured spectra to obtain concentrations of the flavodoxin species.

A second method for measuring redox potentials utilized 5-deaza-FMN as the catalyst for photoreduction (Massey & Hemmerich, 1977) . The same cuvette and indicators were used, and the flavodoxin was mixed with 5-deazaflavin sulfonate (1-5 μM) and the photodonor EDTA (10-15 mM). The cuvette was sealed and made anaerobic as described. The solutions were photoreduced for five to ten second intervals by irradiation with a Sungun, and the solution was allowed to equilibrate for five to ten minutes. Spectra were recorded after the system reached equilibrium. Concentrations of oxidized and reduced components were determined from absorbance spectra.

Redox potentiometry (Dutton, 1978) was employed to obtain data from wild-type flavodoxin and the Asn58Gly mutant at potentials below the the sq/hq midpoint. A spectroelectrochemical cell was constructed (Stankovich, 1980) using a gold foil working electrode and saturated Ag/AgCl counter and reference electrodes. Flavodoxins were mixed with a mediator soup in the cuvette, and the system made anaerobic by cycling between argon and vacuum while stirring, using a glass coated stirbar in the cuvette. The system was poised at decreasing potentials, and spectra were recorded after the potential stabilized. Mediator dyes included indigo disulfonate ($E_{m,7} = -125$ mV), anthraquinone-2,6-disulfonate ($E_{m,7} = -184$ mV), anthraquinone-2-sulfonate ($E_{m,7} = -225$ mV), phenosafranine ($E_{m,7} = -255$ mV), diquat ($E_{m,7} = -350$ mV), benzyl viologen ($E_{m,7} = -350$ mV), methyl viologen ($E_{m,7} = -440$ mV), and triquat ($E_{m,7} = -540$ mV). Concentrations of the dyes were low enough (1-5 μM) that their spectral contributions were insignificant. Concentrations of oxidized, semiquinone, and hydroquinone flavodoxin were determined from absorbance spectra.

Measurement of FMN binding constants

Apoprotein was prepared by dialysis *versus* 2 M KBr at pH 4.0 as described (Entsch & Smillie, 1972) and was redissolved in 100 mM phosphate buffer, 0.5 mM EDTA, at pH 7.0. Free FMN was titrated with apoprotein, and the concentration of bound FMN after each addition was determined from the extent of flavin fluorescence quenching (Curley *et al*., 1991). Binding constants were calculated by quadratic fitting of the data points (Hoover & Ludwig, 1997; Lostao *et al*., 1997), using only the nonlinear portion of the binding curve.

Illustrations

Drawings in Figures 2, 3, 4(b) and 8 were prepared using MOLSCRIPT (Kraulis, 1991); Figures 4(a) and 5 were drawn using MAXIM, made available to us by Dr Mark Rould.

Acknowledgements

This research was supported by NIH grant GM 16429 (M.L.L.) and by Training Grants in Molecular Biophysics, GM 08270 (C.L.D.), and in Cellular and Molecular Biology, GM 07315 (C.H.W.). We are grateful to Dr David P. Ballou for his collaboration in determination of p*K* values by pH jump measurements.

References

Anderson, A. G. & Hermans, J. (1988). Microfolding: conformational probability map for the alanine dipeptide in water from molecular dynamics simulations. *Proteins: Struct. Funct. Genet.* **3**, 262-265.

Anderson, R. F. (1983). Energetics of the one-electron reduction steps of riboflavin, FMN, and FAD to their fully reduced forms. *Biochim. Biophys. Acta,* **722**, 158-162.

Barman, B. & Tollin, G. (1972). Flavine-protein interactions in flavoenzymes. Thermodynamics and kinetics of reduction of *Azotobacter* flavodoxin. *Biochemistry,* **11**, 4755-4759.

Brünger, A. T. (1992). *X-PLOR Version 3.1. A System for X-ray Crystallography and NMR*, Yale University Press, New Haven.

Brünger, A. T., Krukowski, A. & Erickson, J. W. (1990). Slow-cooling protocols for crystallographic refinement by simulated annealing. *Acta Crystallog. sect. A,* **46**, 585-593.

Burkhart, B. M., Ramakrishnan, B., Hongao, Y., Reedstrom, R. J., Markley, J. L., Straus, N. A. & Sundralingam, M. (1995). Structure of the trigonal form of recombinant oxidized flavodoxin from *Anabaena* 7120 at 1.40 Å resolution. *Acta Crystallog. sect. D,* **51**, 318-330.

Caldeira, J., Palma, P., Regalla, M., Lampreia, J., Calvete, J., Schafer, W., Legall, J., Moura, I. & Moura, J. (1994). Primary sequence, oxidation-reduction potentials and tertiary-structure prediction of *Desulfovibrio desulfuricans* ATCC 27774 flavodoxin. *Eur. J. Biochem.* **220**, 987-995.

Cambillau, C. & Horjales, E. (1987). TOM. *J. Mol. Graph.* **5**, 174-177.

Chang, F. C. & Swenson, R. P. (1999). The midpoint potentials for the oxidized-semiquinone couple for Gly57 mutants of the *Clostridium beijerinckii* flavodoxin correlate with changes in the hydrogen bonding interaction with the N(5) proton of the reduced flavin mononucleotide cofactor as measured by NMR chemical shift temperature dependencies. *Biochemistry,* **38**, 7168-7176.

Clubb, R. T., Thanabal, V., Osborne, C. & Wagner, G. (1991). ^{1}H and ^{15}N resonance assignments of oxidized flavodoxin from *Anacystis nidulans* with 3D NMR. *Biochemistry,* **30**, 7718-7730.

Correll, C. C. (1992). Structure determination and analysis of an iron-sulfur flavoprotein: phthalate dioxygenase reductase, PhD thesis, The University of Michigan.

Crespi, H. L., Smith, U., Gajda, L., Tisue, T. & Amerall, R. M. (1972). Characterization of flavodoxin from *S. lividus*. *Bioch. Bioph. Acta,* **256**, 611-618.

Curley, G., Carr, M., Mayhew, S. & Voordouw, G. (1991). Redox and flavin-binding properties of recombinant flavodoxin from *Desulfovibrio vulgaris* (Hildenborough). *Eur. J. Biochem.* **202**, 1091-1100.

Deistung, J. & Thorneley, R. (1986). Electron transfer to nitrogenase. Characterization of flavodoxin from *Azotobacter chroococcum* and comparisons of its redox potentials with those of flavodoxins from *Azotobacter vinlandii* and *Klebsiella pneumoniae* (nifF-gene product). *Biochem. J.* **239**, 69-75.

Dixon, D. A. & Lipscomb, W. N. (1979). Conformations and electronic structures of oxidized and reduced isoalloxazine. *Biochemistry,* **18**, 5770-5775.

Draper, R. D. & Ingraham, L. L. (1968). A potentiometric study of the flavin semiquinone equilibrium. *Arch. Biochem. Biophys.* **125**, 802-808.

Drennan, C. L., Pattridge, K. A., Weber, C. H., Metzger, A. L., Hoover, D. M. & Ludwig, M. L. (1999). Refined structures of oxidized flavodoxin from *Anacystis nidulans*. *J. Mol. Biol.* **294**, 711-724.

Dutton, L. (1978). Redox potentiometry: determination of midpoint potentials of oxidation-reduction components of biological electron-transfer systems. *Methods Enzymol.* **54**, 411-435.

Entsch, B. & Smillie, R. M. (1972). Oxidation-reduction properties of phytoflavin, a flavoprotein from blue-green algae. *Arch. Bioch. Biophys.* **151**, 378-386.

Franken, H., Rüterjans, H. & Müller, F. (1984). Nuclear-magnetic-resonance investigation of ^{15}N-labeled flavins, free and bound to *Megasphaera elsdenii* apoflavodoxin. *Eur. J. Biochem.* **138**, 481-489.

Fukuyama, K., Matsubara, H. & Rogers, L. J. (1992). Crystal structure of oxidized flavodoxin from a red alga *Chondrus crispus* refined at 1.8 Å resolution. Description of the flavin mononucleotide binding site. *J. Mol. Biol.* **225**, 775-789.

Hall, L. H., Bowers, M. L. & Durfor, C. N. (1987a). Further consideration of flavin coenzyme biochemistry afforded by geometry-optimized molecular orbital calculations. *Biochemistry,* **26**, 7401-7409.

Hall, L. H., Orchard, B. J. & Tripathy, S. K. (1987b). The structure and properties of flavins: molecular orbital study based on totally optimized geometries. I. Molecular geometry investigations. *Internat. J. Quant. Chem.* **31**, 195-216.

Hall, L. H., Orchard, B. J. & Tripathy, S. K. (1987c). The structure and properties of flavins: molecular orbital study based on totally optimized geometries. II. Molecular orbital structure and electron distribution. *Internat. J. Quant. Chem.* **31**, 217-242.

Honig, B. & Nicholls, A. (1995). Classical electrostatics in biology and chemistry. *Science,* **268**, 1144-1149.

Hoover, D. M. & Ludwig, M. L. (1997). A flavodoxin that is required for enzyme activation: the structure of oxidized flavodoxin from *Escherichia coli* at 1.8 Å resolution. *Protein Sci.* **6**, 2525-2537.

Howard, A. J., Nielsen, C. & Xuong, N. H. (1985). Software for a diffractometer with multiwire area detector. *Methods Enzymol.* **114**, 452-472.

Hutchinson, E. G. & Thornton, J. M. (1994). A revised set of potentials for beta turn formation in proteins. *Protein Sci.* **3**, 2207-2216.

Jones, T. A. & Thirup, S. (1986). Using known substructures in protein model building and crystallography. *EMBO J.* **5**, 819-822.

Klugkist, J., Voorberg, J., Haaker, H. & Veeger, C. (1986). Characterization of three different flavodoxins from *Azotobacter vinelandii*. *Eur. J. Biochem.* **155**, 33-40.

Kraulis, P. J. (1991). MOLSCRIPT: a program to produce both detailed and schematic plots of protein structure. *J. Appl. Crystallog.* **24**, 946-950.

Lostao, A., Gomez-Moreno, C., Mayhew, S. G. & Sancho, J. (1997). Differential stabilization of the three FMN redox forms by tyrosine 94 and tryptophan 57 in flavodoxin from *Anabaena* and its influence on the redox potentials. *Biochemistry,* **36**, 14334-14344.

Ludwig, M. L. & Luschinsky, C. L. (1992). Structure and redox properties of clostridial flavodoxin. In *Chemistry and Biochemistry of Flavoenzymes* (Muller, F., ed.), vol. 3, pp. 427-466, CRC Press, Boca Raton.

Ludwig, M. L., Burnett, R. M., Darling, G. D., Jordan, S. R., Kendall, D. S. & Smith, W. W. (1976). The structure of *Clostridium MP* flavodoxin as a function of oxidation state: some comparisons of the FMN-binding sites in oxidized, semiquinone, and reduced forms. In *Flavins and Flavoproteins* (Singer, T. P., ed.), pp. 393-404, Elsevier, Amsterdam.

Ludwig, M. L., Schopfer, L. M., Metzger, A. L., Pattridge, K. A. & Massey, V. (1990). Structure and oxidation-reduction behavior of 1-deaza-FMN flavodoxins: modulation of redox potentials in flavodoxins. *Biochemistry,* **29**, 10364-10375.

Ludwig, M. L., Pattridge, K. A., Metzger, A. L., Dixon, M. M., Eren, M., Feng, Y. & Swenson, R. P. (1997). Control of oxidation-reduction potentials in flavodoxin from *Clostridrium beijerinckii*: the role of conformation changes. *Biochemistry,* **36**, 1259-1280.

Luschinsky, C. L., Dunham, W. R., Osborne, C., Pattridge, K. A. & Ludwig, M. L. (1991). Structural analysis of fully reduced *A. nidulans* flavodoxin. In *Flavins and Flavoproteins 1990* (Curti, B., Ronchi, S. & Zanetti, G., eds), pp. 409-413, Walter de Gruyter, Berlin.

Massey, V. (1991). A simple method for the determination of redox potentials. In *Flavins and Flavoproteins 1990* (Curtis, B., Roncho, S. & Zanetti, G., eds), pp. 59-66, Walter de Gruyter, Berlin.

Massey, V. & Hemmerich, P. (1977). A photochemical procedure for reduction of oxidation-reduction proteins employing deazariboflavin as catalyst. *J. Biol. Chem.* **252**, 5612-5614.

Mayhew, S. (1971). Studies on flavin binding in flavodoxins. *Biochim. Biophys. Acta,* **235**, 289-302.

Mayhew, S. G. & Tollin, G. (1992). General properties of flavodoxins. In *Chemistry and Biochemistry of Flavoenzymes* (Müller, F., ed.), vol. 3, pp. 389-426, CRC Press, Boca Raton.

Mayhew, S. G., Foust, G. P. & Massey, V. (1969). Oxidation-reduction properties of flavodoxin from *Peptostreptococcus elsdenii*. *J. Biol. Chem.* **244**, 803-810.

Mayhew, S. G., O'Connell, D. P., O'Farrell, P. A., Yalloway, G. N. & Geoghegan, S. M. (1996). Regulation of the redox potentials of flavodoxins: modification of the flavin binding site. *Biochem. Soc. Trans.* **24**, 122-127.

Moonen, C. T. W., Vervoort, J. & Müller, F. (1984). A reinvestigation of the structure of oxidized and reduced flavin. Carbon-13 and nitrogen-15 nuclear magnetic resonance study. *Biochemistry,* **23**, 4859-4867.

Munoz, V. & Serrano, L. (1994). Intrinsic secondary structure propensities of the amino acids, using statistical phi-psi matrices: comparison with experimental scales. *Proteins: Struct. Funct. Genet.* **20**, 301-311.

O'Farrell, P. A., Walsh, M. A., McCarthy, A. A., Higgins, T. M., Voordouw, G. & Mayhew, S. G. (1998). Modulation of the redox potentials of FMN in *Desulfovibrio vulgaris* flavodoxin: thermodynamic properties and crystal structures of glycine-61 mutants. *Biochemistry,* **37**, 8405-8416.

Olsen, D. B., Sayers, J. R. & Eckstein, F. (1993). Site-directed mutagenesis of single-stranded and double-stranded DNA by phosphorothioate approach. *Methods Enzymol.* **217**, 189-217.

Paulsen, K. E., Stankovich, M. T., Stockman, B. J. & Markley, J. L. (1990). Redox and spectral properties of flavodoxin from *Anabaena* 7120. *Arch. Biochem. Biophys.* **280**, 68-73.

Pueyo, J. J., Gomez-Moreno, C. & Mayhew, S. G. (1991). Oxidation-reduction potentials of ferredoxin-$NADP^+$ reductase and flavodoxin from *Anabaena* PCC 7119 and their electrostatic and covalent complexes. *Eur. J. Biochem.* **202**, 1065-1071.

Ramachandran, G. N. & Sasisekharan, V. (1968). Conformation of polypeptides and proteins. *Advan. Protein Chem.* **28**, 283-437.

Rao, S., Shaffie, F., Yu, C., Satyshur, K., Stockman, B., Markley, J. & Sundarlingam, M. (1992). Structure of the oxidized long-chain flavodoxin from *Anabaena* 7120 at 2 Å resolution. *Protein Sci.* **1**, 1413-1427.

Richardson, J. S. (1981). The anatomy and taxonomy of protein structure. *Advan. Protein Chem.* **34**, 167-339.

Romero, A., Caldeira, J., LeGall, J., Moura, I., Moura, J. J. G. & Romao, M. J. (1996). Crystal structure of flavodoxin from *Desulfovibrio desulfuricans* ATCC 27774 in two oxidation states. *Eur. J. Biochem.* **239**, 190-196.

Sayers, J. R., Schmidt, W. & Eckstein, F. (1988). 5′-3′ exonucleases in phosphorothioate-based oligonucleotide-directed mutagenesis. *Nucl. Acids Res.* **16**, 791-802.

Scully, J. & Hermans, J. (1994). Backbone flexibility and stability of reverse turn conformation in a model system. *J. Mol. Biol.* **235**, 682-694.

Sevrioukova, I., Shaffer, C., Ballou, D. P. & Peterson, J. A. (1996). Equilibrium and transient state spectrophotometric studies of the mechanism of reduction of the flavoprotein domain of P450BM-3. *Biochemistry,* **35**, 7058-7068.

Smith, W. W., Burnett, R. M., Darling, G. D. & Ludwig, M. L. (1977). Structure of the semiquinone form of flavodoxin from *Clostridium MP*. *J. Mol. Biol.* **117**, 195-225.

Stankovich, M. T. (1980). An anaerobic spectroelectrochemical cell for studying the spectral and redox properties of flavoproteins. *Anal. Biochem.* **109**, 295-308.

Steensma, E., Heering, H. A., Hagen, W. R. & van Mierlo, C. P. M. (1996). Redox properties of wild-type, Cys69Ala, and Cys69Ser *Azotobacter vinelandii* flavodoxin II as measured by cyclic voltammetry and EPR spectroscopy. *Eur. J. Biochem.* **235**, 167-172.

Stockman, B. J., Westler, W. M., Mooberry, E. S. & Markley, J. L. (1988). Flavodoxin from *Anabaena* 7120: uniform nitrogen-15 enrichment and hydrogen-1, nitrogen-15, and phosphorus-31 NMR investigations of the flavin mononucleotide binding site

in the reduced and oxidized states. *Biochemistry,* **27**, 136-142.

Swenson, R. P. & Krey, G. D. (1994). Site-directed mutagenesis of tyrosine-98 in the flavodoxin from *Desulfovibrio vulgaris* (Hildenborough): regulation of oxidation-reduction properties of the bound FMN cofactor by aromatic, solvent, and electrostatic interactions. *Biochemistry,* **33**, 8505-8514.

Sykes, G. A. & Rogers, L. J. (1984). Redox potentials of algal and cyanobacterial flavodoxins. *Biochem. J.* **217**, 845-850.

Taylor, M. F., Boylan, M. H. & Edmondson, D. E. (1990). *Azotobacter vinelandii* flavodoxin: purification and properties of the recombinant, dephospho form expressed in *Escherichia coli*. *Biochemistry,* **29**, 6911-6918.

Vervoort, J., Müller, F., Mayhew, S. G., van den Berg, W. A. M., Moonen, C. T. W. & Bacher, A. (1986). A comparative carbon-13, nitrogen-15, and phosphorus-31 nuclear magnetic resonance study on the flavodoxins from *Clostridium MP, Megasphaera elsdenii,* and *Azotobacter vinelandii*. *Biochemistry,* **25**, 6789-6799.

Vetter, H. J. & Knappe, J. (1971). Flavodoxin and ferredoxin of *Escherichia coli*. *Hoppe-Seyler's Z. Physiol. Chem.* **352**, 433-446.

Watenpaugh, K., Sieker, L. & Jensen, L. (1973). The binding of riboflavin-5′-phosphate in a flavoprotein: flavodoxin at 2.0-Angstrom resolution. *Proc. Natl Acad. Sci. USA,* **70**, 3857-3860.

Watt, W., Tulinsky, A., Swenson, R. P. & Watenpaugh, K. D. (1991). Comparison of the crystal structures of a flavodoxin in its three oxidation states at cryogenic temperatures. *J. Mol. Biol.* **218**, 195-208.

Xuong, N. H., Nielsen, C., Hamlin, R. & Anderson, D. (1985). Strategy for data collection from protein crystals using a multiwire counter area detector diffractometer. *J. Appl. Crystallog.* **18**, 342-350.

Yalloway, G. N., Mayhew, S. G., Malthouse, J. P. G., Gallagher, M. E. & Curley, G. P. (1999). pH-dependent spectroscopic changes associated with the hydroquinone of FMN in flavodoxins. *Biochemistry,* **38**, 3753-3762.

Yang, A.-S., Hitz, B. & Honig, B. (1996). Free energy determinants of secondary structure formation. β-turns and their role in protein folding. *J. Mol. Biol.* **259**, 873-882.

Yoch, D. C. (1972). The electron transport system in nitrogen fixation by azotobacter. IV. Some oxidation-reduction properties of azotoflavin. *Biochem. Biophys. Res. Commun.* **49**, 335-342.

Zheng, Y.-J. & Ornstein, R. L. (1996). A theoretical study of the structures of flavin in different oxidation and protonation states. *J. Am. Chem. Soc.* **118**, 9402-9408.

Zhou, Z. & Swenson, R. P. (1995). Electrostatic effects of surface acidic amino acid residues on the oxidation-reduction potentials of the flavodoxin from *Desulfovibrio vulgaris* (Hildenborough). *Biochemistry,* **34**, 3183-3192.

Zhou, Z. & Swenson, R. P. (1996a). The cumulative electrostatic effect of aromatic stacking interactions and the negative electrostatic environment of the flavin mononucleotide binding site is a major determinant of the reduction potential for the flavodoxin from *Desulfovibrio vulgaris* [Hildenborough]. *Biochemistry,* **35**, 15980-15988.

Zhou, Z. & Swenson, R. P. (1996b). Evaluation of the electrostatic effect of the 5′-phosphate of the flavin mononucleotide cofactor on the oxidation-reduction potentials of the flavodoxin from *Desulfovibrio vulgaris* (Hildenborough). *Biochemistry,* **35**, 12443-12454.

Edited by R. Huber

(Received 15 January 1999; received in revised form 20 August 1999; accepted 20 August 1999)